



Università  
Ca' Foscari  
Venezia

**Dipartimento  
di Scienze Ambientali  
Informatica e Statistica**

# Technical Report Series

## Rapporto di Ricerca

DAIS-2012-3

A. Albarea

Statistical analysis of Italian earthquake  
catalogue 1600 - 2003

# Statistical analysis of Italian earthquake catalogue 1600 - 2003\*

Andrea Albarea

Department of Environmental Science, Informatics and Statistics  
Ca' Foscari University of Venice

August 30, 2012

## 1 Introduction

Earthquake catalogues are an historical memory of seismology that contains the main characteristics of shocks like time, magnitude and epicenter coordinates. These catalogues are very important because they allow to study the past seismic events of a reference region. Here we study an Italian catalogue from 1600 to 2003 and report results based on statistical data depth. With this method we want to measure the seismic risk. Small (Small, 1990) first advocated the use of data depth to study the spatial distribution of earthquake epicenters on the Earth' surface. His suggestion was meant as an illustration of data depth of directional data because epicenters can be represented as points on the surface of a sphere. In this work, first, we illustrate the general features of the Italian earthquake catalogue together with the results of preliminary descriptive analysis. After that we introduce the concept of data depth and provide a map of seismic risk for Italy using the depth centrality ordering (Liu et al, 1999). Finally, we include in the analysis the intensity of earthquakes with the goal to obtain a comprehensive investigation of the data.

---

\*Research project *Statistical analysis of historical earthquake catalogues*, supervisor M. Romanazzi. Financial support by DAIS, research funds of M. Romanazzi and PRIN 2008 research project *Approximate likelihood methods for high-dimensional dependencies*, coordinator P. Vidoni

## 2 Italian earthquake catalogue 1600 - 2003

In this work we consider a catalogue of Italian earthquakes during the period 1600 – 2003 <sup>1</sup>. The total number of recorded events is 1469. Variables included in the catalogue are:

- TIME: occurrence time for each shock
- LATITUDE, LONGITUDE: geographical coordinates of epicenters of the catalogue
- INTENSITY: ( $M_w$ ) magnitude (only shocks with magnitude not less than 4.5 are included in the catalogue)
- LABEL: tectonic region of the shock; there are 8 tectonic regions roughly covering Italy and coastal portions of nearby seas
  1. MR1, Western Alps
  2. MR2, Eastern Alps
  3. MR3, Central Northern Apennines Alps
  4. MR4, Central Northern Apennines West
  5. MR5, Southern Apennines Apulia
  6. MR6, Southern Apennines
  7. MR7, Calabrian Arc
  8. MR8, Sicily

Some epicenters located in the sea or outside Italian borders are included in the dataset because they belong to tectonic regions considered in the list above.

The most commonly used class of magnitude scales, following from Richter's original local magnitude scale, is based on the logarithm of the amplitude of the recorded seismic waves. Local magnitude, denoted  $M_l$ , is arbitrarily defined based on the maximum observed amplitude on a Wood-Anderson seismometer, with a period of 0.8 sec, recorded at 100 km from the earthquake. In practice, of course, the recording distance is not exactly 100 km, and corrections must be made to account for amplitude changes with distance due to attenuation and geometrical spreading. Station corrections are usually determined, to account for site conditions. Corrections must also be made for recordings on instruments other than the now-obsolete Wood-Anderson. Local magnitudes are best suited to small local earthquakes with predominately high-frequency energy (Richter, 1935) and (Hutton et al, 2010).

Other scales have been developed that are based on the logarithm of the amplitude of a particular phase, the most common being two scales for teleseismic (global) recordings: the body wave magnitude,  $M_b$ , based on body waves with periods of several seconds (Gutenberg and Richter, 1956), and the surface wave magnitude,  $M_s$ , based on 20 second surface waves (Gutenberg and Richter, 1956). These magnitude scales are

---

<sup>1</sup>Data set kindly provided by Basili, R. and Rotondi, R.

used for most globally-recorded earthquakes, but are not appropriate for the largest earthquakes, those of magnitude greater than 7 or 8. This is because the energy at high frequencies saturates for large events, e.g. the 1 second energy radiated by a magnitude 8 earthquake is similar to the 1 second energy radiated by a magnitude 7 earthquake. The body wave and surface wave magnitudes therefore saturate at around magnitude 7 to 8. Therefore, some of the largest earthquakes in a catalogue may be of much higher magnitude than reported.

The moment magnitude,  $M_w$ , scale (Hanks and Kanamori, 1979) is based on the logarithm of the moment of the earthquake, rather than on the amplitude of a particular phase at a particular frequency, and therefore has the advantage that it does not saturate for large magnitudes. The seismic moment of an earthquake is usually estimated by fitting a double couple moment tensor solution to the recorded waveforms from the earthquake. Alternatively, for well-recorded earthquakes, the moment can be estimated from a finite source model of the earthquake (Woessner et al, 2010).

### 3 Preliminary descriptive analysis

In this section we report the main results of preliminary descriptive analysis. Table 1 shows the distribution of earthquakes by tectonic zones. Regions with highest frequency of epicenters are no. 4 and no. 3, respectively.

Region	%	Region	%
1: Western Alps	7.35	5: Southern Apennines Apulia	6.06
2: Eastern Alps	14.64	6: Southern Apennines	6.13
3: Central Northern Apennines Alps	17.49	7: Calabrian Arc	12.93
4: Central Northern Apennines West	26.07	8: Sicily	9.33

Table 1: Distribution of Italian earthquakes 1600 – 2003 ( $M_w \geq 4.5$ ) according to tectonic region.

Boxplots in Figure 1 show the distribution of earthquake magnitude by tectonic region. We test the equality of means of tectonic zones and we reject the null hypothesis of mean equality, as the p-value of the F-statistic is very low. This result is confirmed by the notches drawn in Figure 1. Higher earthquakes occurred in the South of country, in fact their medians are greater than in the North of Italy. Table 2 reports the summary statistics of Figure 1.

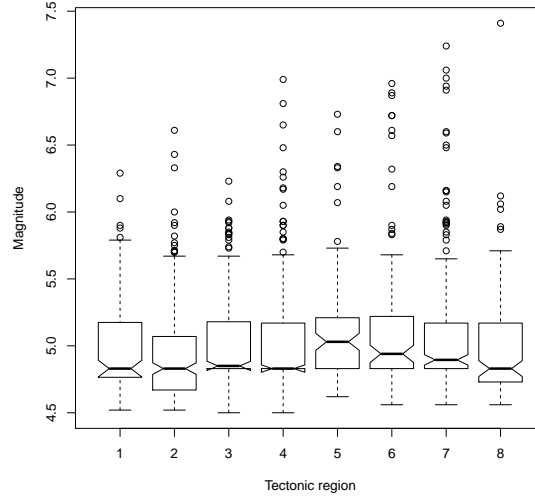


Figure 1: Boxplot of earthquake magnitude by tectonic region.

Region	Magnitude					
	Min	1.st Quartile	Median	Mean	3.rd Quartile	Max
1	4.520	4.768	4.830	4.997	5.173	6.290
2	4.520	4.670	4.830	4.954	5.070	6.610
3	4.500	4.830	4.850	5.004	5.180	6.230
4	4.500	4.830	4.830	4.990	5.170	6.990
5	4.620	4.830	5.030	5.098	5.210	6.730
6	4.560	4.830	4.940	5.164	5.215	6.960
7	4.560	4.830	4.895	5.110	5.170	7.240
8	4.560	4.730	4.830	5.017	5.170	7.410
Italy	4.500	4.810	4.830	5.023	5.170	7.410

Table 2: Summary statistics of earthquake magnitude by tectonic region.

The histogram in Figure 2 shows that most Italian earthquakes are not so strong, indeed the mean and median magnitude are 5.023 and 4.830, respectively. During the reference period there were few earthquakes with great intensity and the most revealing occurred in the South of Italy. For example, magnitude quantile at 95% is equal to 5.85, it means that just 5% of earthquakes have a magnitude higher than 5.85.

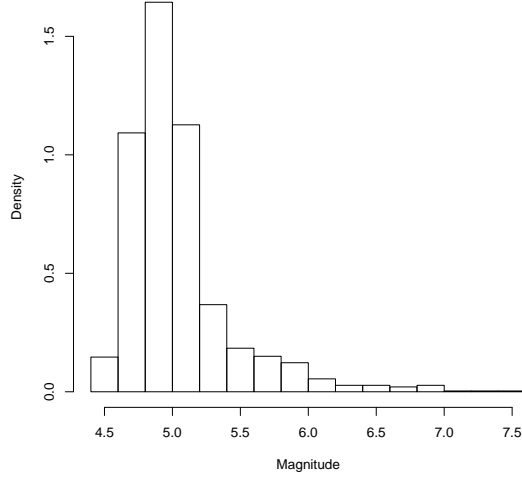


Figure 2: Magnitude distribution.

The time series of recorded shocks and their magnitude is shown in the top panel of Figure 3. An increase of the number of recorded events with time is clear, in particular in the lower range of magnitude. This is confirmed by Table 4 which shows in detail the frequency distribution of events during the four centuries covered by the catalogue. An explanation is that in the past centuries they did not have automatic devices able to properly measure earthquake intensity, thus shocks were classified according to observed damages and many shocks with lower intensity probably were not recorded. The lower panel of Figure 3 shows earthquakes with magnitude greater than 6.5. The most important shock occurred in 1693 near Noto, a town situated in the east of Sicily, with moment magnitude 7.41. The second greatest earthquake, with  $M_w = 7.24$ , happened in 1908 between Messina and Reggio Calabria. This shock was also the most catastrophic in terms of human deaths, with about 100.000 victims. Another two earthquakes with moment magnitude greater than 7.0 occurred in Lamezia Terme, luckily with consequences less disastrous than the first two cited above.

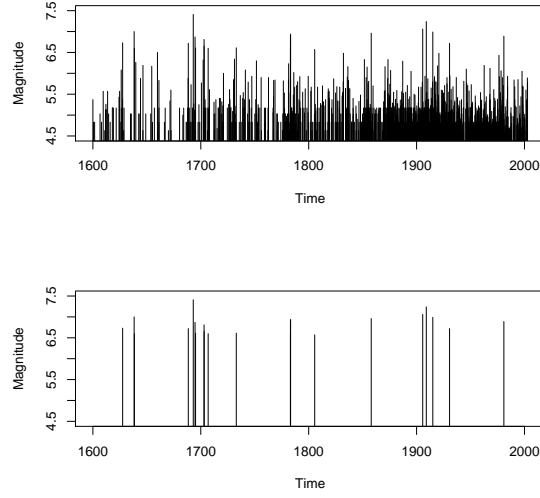


Figure 3: Time series of earthquake magnitude. Top: all events; bottom: events with magnitude greater than 6.5.

Time	%
[1600-1700]	5.24
(1700-1800]	11.71
(1800-1900]	27.77
(1900-2003]	55.28

Table 3: Distribution of Italian earthquakes 1600 – 2003 ( $M_w \geq 4.5$ ) by century.

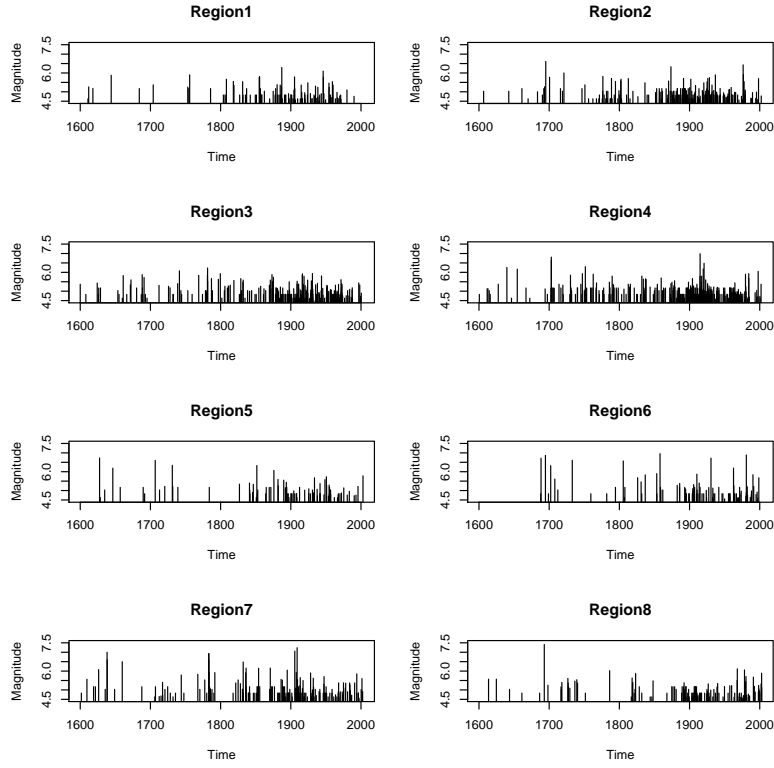


Figure 4: Time series of earthquake magnitude by tectonic region.

Tables 4 and 5 report the conditional distributions of magnitude classes given the region and the conditional distributions of regions given magnitude class, respectively. The latter shows that region no. 4 always has the highest frequency of events, for all magnitude classes. Magnitude classes correspond to quartiles and in the upper class, including the biggest earthquakes, regions no. 3 and no. 4 are in the first two positions.



Region	Magnitude			
	[4.5-4.81] %	(4.81-4.83] %	(4.83-5.17] %	(5.17-7.41] %
1	26.85(29)	30.56(33)	17.59(19)	25.00(27)
2	34.42(74)	20.47(44)	31.16(67)	13.95(30)
3	24.90(64)	24.12(62)	25.68(66)	25.29(65)
4	23.76(91)	28.72(110)	31.33(120)	16.19(62)
5	17.98(16)	23.60(21)	32.58(29)	25.84(23)
6	16.67(15)	31.11(28)	25.56(23)	26.67(24)
7	21.58(41)	27.37(52)	27.37(52)	23.68(45)
8	27.74(38)	24.09(33)	23.36(32)	24.82(34)

Table 4: Conditional distribution of magnitude by region. Class extremes are quartiles and numbers in parentheses are absolute frequencies.

Region	Magnitude			
	[4.5-4.81] %	(4.81-4.83] %	(4.83-5.17] %	(5.17-7.41] %
1	7.88(29)	8.62(33)	4.66(19)	8.71(27)
2	20.11(74)	11.49(44)	16.42(67)	9.68(30)
3	17.39(64)	16.19(62)	16.18(66)	20.97(65)
4	24.73(91)	28.72(110)	29.41(120)	20.00(62)
5	4.35(16)	5.48(21)	7.11(29)	7.42(23)
6	4.08(15)	7.31(28)	5.64(23)	7.74(24)
7	11.14(41)	13.58(52)	12.57(52)	14.52(45)
8	10.33(38)	8.62(33)	7.84(32)	10.97(34)

Table 5: Conditional distribution of regions by magnitude. Layout as in Table 4.

The joint analysis of time, intensity and tectonic region reported in Table 8 confirms the foregoing. Just the biggest earthquakes were detected during the first two centuries and for each time interval the most seismically active regions are the no. 4, Central Northern Apennines West, and no. 3, Southern Apennines Apulia. Pearson's chi-squared test rejects the null hypothesis of independence of the three variables, indeed the p-value is very close to 0.

In seismology waiting (or inter event) time is defined to be the time elapsed between consecutive earthquakes in a given region. We report a few results involving the overall distribution and the region-conditional distributions. Figure 5 represents the waiting-time distribution for all the earthquakes in the catalogue. The distribution is decreasing, with the major part of consecutive earthquakes occurring within less than a year. For example, the median waiting-time is equal to 0.72. There are also cases where a shock comes in succession to another after a long period of time, like 10 or more years, mostly in the period 1600 - 1800 when many earthquakes with low magnitude were not recorded.

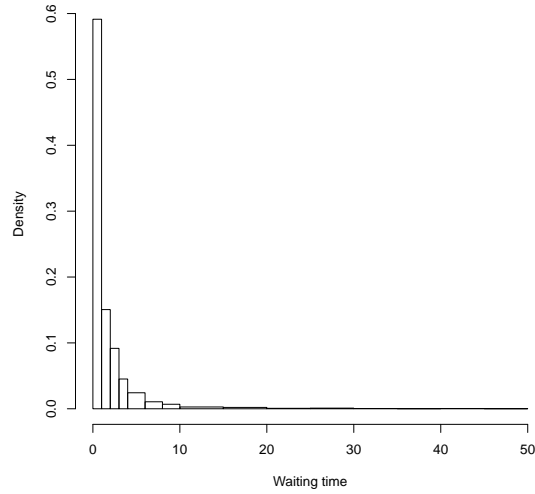


Figure 5: Waiting-time distribution.

Figure 6 and Table 6 report the summary statistics of the waiting-time conditional on tectonic zone. As suggested by the Omori's law and Gutenberg-Richter law, regions with lower waiting-time are those with a higher seismic activity (no. 4 and no. 3). Instead, Southern Apennines Apulia (no. 5) has waiting-time higher than the others, with a median (2.08) almost three times the overall median (0.72), which suggests Southern Apennines Apulia to have a lower seismic activity. Similar considerations apply to regions no. 1 and no. 6, but with less pronounced differences. These differences are confirmed by the empirical distribution function of waiting-time for each region (Figure 7) and by p-values of Kolmogorov-Smirnov test (Table 7) between tectonic regions considered above.

Region	Waiting-time					
	Min	1.st quartile	Median	Mean	3.rd quartile	Max
1	0.0214	0.5737	1.3090	3.5430	3.1960	49.2000
2	0.0027	0.3194	0.7839	1.8480	1.7620	35.8100
3	0.0004	0.2623	0.6747	1.5640	1.6480	24.7800
4	0.0017	0.1571	0.3881	1.0510	0.8916	21.8300
5	0.0617	0.5597	2.0770	4.2640	4.5890	44.7500
6	0.0274	0.5688	1.4740	3.4900	3.9360	26.4700
7	0.0007	0.3101	0.8790	2.1200	2.5920	27.9000
8	0.0059	0.3703	0.9991	2.8610	2.3310	34.6100
Italy	0.0004	0.2735	0.7232	2.0890	2.0710	49.2000

Table 6: Summary statistics of waiting-time by tectonic region.

Region								
	1	2	3	4	5	6	7	8
1		0.01063	0.0002627	$2.755e-11$	0.11	0.4573	0.04379	0.1706
2			0.4844	$9.549e-07$	$1.031e-05$	0.000586	0.1962	0.1973
3				$2.869e-05$	$1.511e-05$	$1.475e-05$	0.03722	0.02517
4					$1.9e-10$	$4.191e-11$	$2.837e-08$	$4.117e-08$
5						0.8702	0.009746	0.005214
6							0.01855	0.06022
7								0.7177
8								

Table 7: P-value of Kolmogorov-Smirnov test of waiting-time between tectonic regions.

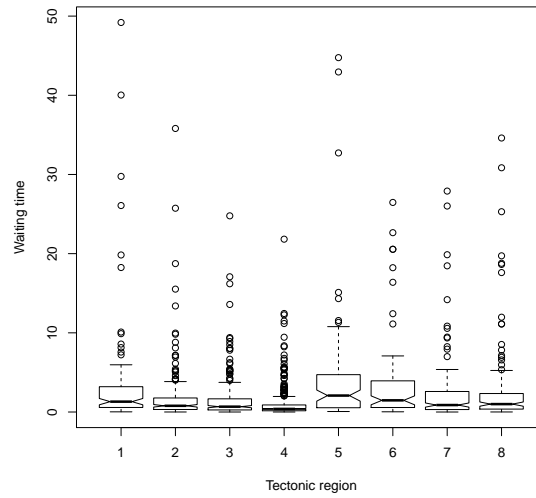


Figure 6: Boxplots of waiting-time by tectonic region.

## CUMULATIVE DISTRIBUTION FUNCTION OF WAITING TIME

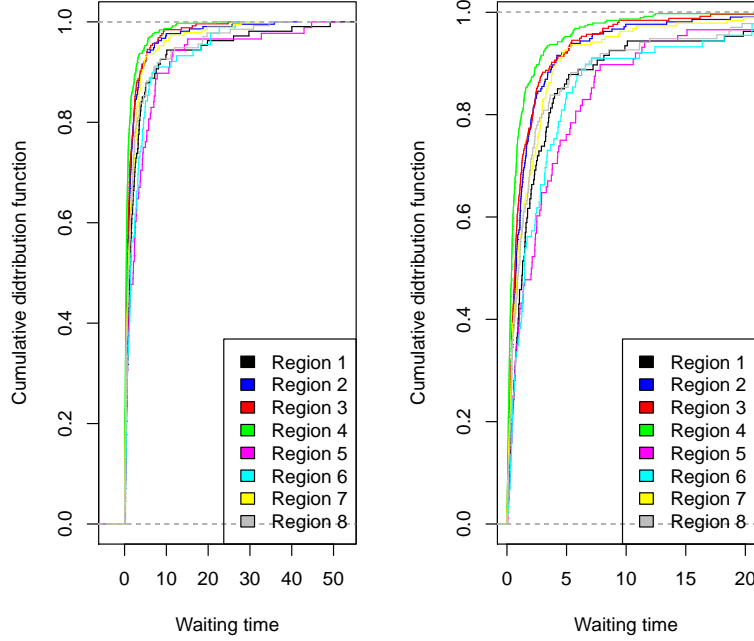


Figure 7: Cumulative distribution function of waiting-time by tectonic region. Left: entire graphic; right: time not greater than 20 years.

To describe the *local* behavior of seismic activity, we consider the time trajectories representing an historical trend of seismic activity in a circular area, or neighbourhood, around a given station. The radius of the neighbourhood was euristically chosen as the 5% quantile (0.65) of the distribution of pairwise distances between epicenters. If the distance between the station and an epicenter is lower than this threshold, then the corresponding event is considered to belong to the neighbourhood of the station, otherwise it is discarded. The province capitals are taken as test stations.

Figure 8 shows the trajectories of L'Aquila, Messina, Forlì and Rome, the first three cities well known for nearby seismic activity, the latter with much lower nearby seismic activity. The results agree with the analysis made earlier. L'Aquila and Messina are characterized by a frequent seismic activity including earthquakes of great intensity, also Forlì but a less extent with respect to the other two cities.

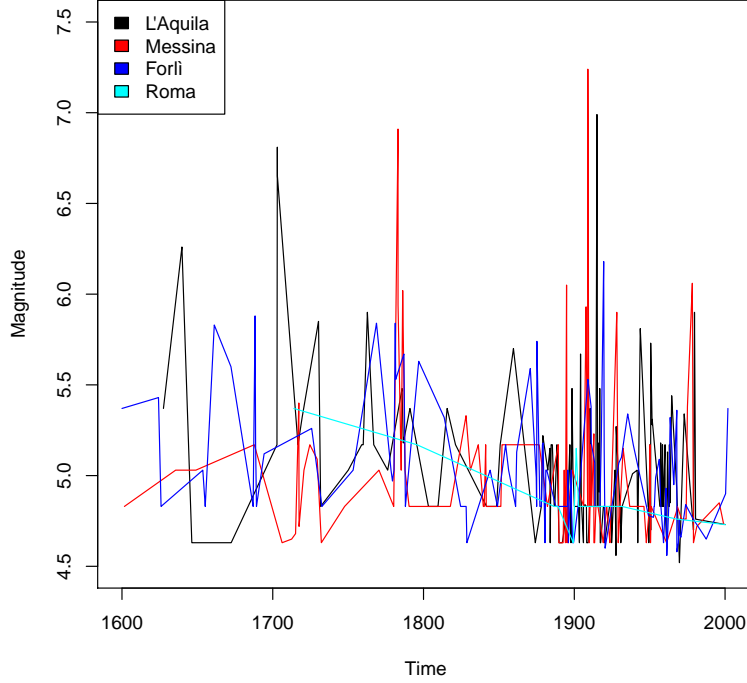


Figure 8: Trajectories of earthquakes of 4 Italian cities.

## 4 Data Depth

Data Depth (DD) is a statistical method to rank the points of a space according to centrality with respect to an assumed probability distribution or a data set. Usually, reference space is the Euclidean space  $\mathbb{R}^p$ , i.e., Data Depth is multivariate in nature, univariate case is obtained as a particular case. Through the application of a ranking function (depth function) each point of the space receives a non negative score describing its degree of centrality (depth value). Depth implicitly defines a center as the point with maximum depth value, and decreases along any direction from the center.

**Definition 1 (Depth Function)** *A depth function  $d(\cdot)$  measures the centrality of a point with respect to a probability distribution  $F$  or a data set. It is a function from the Euclidean space  $\mathbb{R}^p$  into the set of non negative real numbers, that is  $d : x \in \mathbb{R}^p \rightarrow d(x; F) \geq 0, x \rightarrow d(x; F)$ .*

A depth function should satisfy the following properties:

1. affine invariance:  $d(x; F) = d(Ax + b; F_{A,b})$ ;

2. monotonicity relative to deepest point: depth decreases along the rays from the center;
3.  $F$  centro-symmetric about  $c \implies d(x; F) \leq d(c; F)$  for all  $x$ ;
4. if  $\|x\| \rightarrow \infty \implies d(x; F) \rightarrow 0$ ;

Commonly used depth functions include Mahalanobis' and other depth functions (Liu et al, 1999) also with extensions to directional and functional data. Geometrical depth functions are nonparametric and use simple geometrical structures (e.g., simplices, halfspaces) to capture information about reference distribution or data set and with respect to Mahalanobis' depth are data adaptive. In fact, the contours of simplicial and halfspace depth tend to follow the structure of data, while the contours of Mahalanobis' depth are always ellipsoids independently of the structure of data. The main trouble for halfspace and simplicial depth can occur in high dimension because of information sparsity.

Two examples of depth-based functionals are:

- location functional: maximizer of the depth function, that is the deepest point of the space with respect to the distribution;
- dispersion functional: Lebesgue integral of the depth function.

Depth-based functionals are devised in the general multivariate situation and they have the advantage of simple geometrical interpretations.

**Definition 2 (Depth-based location)** *For a depth function  $d(\cdot)$ , the location parameter (or multivariate median) of the distribution is*

$$\theta(F) = \operatorname{argmax}_x d(x; F)$$

*and the corresponding sample statistic is*

$$\theta(\hat{F}_n) = \operatorname{argmax}_x d(x; \hat{F}_n).$$

Depth-based medians are important because they provide nonparametric and remarkably robust multivariate estimators of location. A general dispersion parameter is the (Lebesgue) integral of  $d(x; F)$

$$\gamma_F = \int_{\mathbb{R}^p} d(x; F) dx. \quad (1)$$

Here we concentrate on simplicial depth  $d_S(\cdot; F)$ , defined to be the probability coverage of random simplices. A random simplex  $S_{p+1}^{(F)} \equiv S_{p+1}^{(F)}(X_1, \dots, X_{p+1})$  is the convex hull of  $p+1$  random observations  $X_i, i = 1, \dots, p+1$  from the probability distribution  $F$ .

**Definition 3 (Simplicial depth)** *Let  $F$  be a probability distribution and let  $\mathcal{S}_{p+1}^{(F)}$  be the class of random simplices of  $\mathbb{R}^p$  from  $F$ . For  $x \in \mathbb{R}^p$*

$$d_S(x; F) = P_F(S_{p+1}^{(F)} \in \mathcal{S}_{p+1}^{(F)} : x \in S_{p+1}^{(F)}). \quad (2)$$

At the beginnings of data depth it was almost a postulate that depth ranks could single out just one center of a distribution, corresponding to the maximizer of the ranks, whatever the shape of the distribution, unimodal or multimodal. A new concept of depth, called local depth, shows that some generalized depth functions can indeed account for multimodal data, having multiple centers. Local depth measures centrality conditional on a bounded neighbourhood of each point of the space. These generalizations are called local depth functions because they consider just the behavior of the probability distribution in a nearby region of the point under consideration, instead of the entire space.

A local version  $ld_S(\cdot; F, \tau)$  of simplicial depth is obtained by constraining the size of simplices not to exceed a given size  $\tau > 0$  (Agostinelli and Romanazzi, 2011). Suitable measures  $t(S_{p+1}^{(F)})$  of size are diameter or volume.

**Definition 4 (Local simplicial depth)** *Let the notation be as in Definition 3. For a given  $\tau > 0$ ,*

$$ld_S(x; F, \tau) = P_F(S_{p+1}^{(F)} \in \mathcal{S}_{p+1}^{(F)} : x \in S_{p+1}^{(F)} \cap t(S_{p+1}^{(F)}) \leq \tau). \quad (3)$$

**Remark 5** *In the univariate case, it is easily shown (Agostinelli and Romanazzi, 2011) that, when  $\tau \rightarrow \infty$ ,  $ld_S(x; F, \tau)$  converges to  $d_S(x; F)$ ,  $x \in \mathbb{R}^p$ . Hence, in this case, local depth can be considered a family of (generalized) depth functions, indexed by  $\tau$ , and the family includes global depth.*

The  $\tau$  parameter dictates the width of the neighbourhood around each point of the space. It is similar to the bandwidth, or window size, in kernel density estimation (Rosenblatt, 1956). Since it is constant in the whole of the space, local depth ranks (like depth rank) can be used to order data points according to centrality.

## 5 Results

### 5.1 Spatial Analysis

In the following analysis empirical simplicial depth is define to be the proportion of simplices including a point  $x$ , where the shape of simplices depends on the dimension. For Example, when studying the spatial distribution of earthquakes, simplices are triangles with vertices corresponding to epicenters and for the Italian catalogue there are  $\binom{1469}{3}$  such triangles. The empirical simplicial depth is the proportion of sample simplices including in a given station. This is the reason data depth analysis can produce a measures of seismic risk. In fact, the depth value of a station under consideration is exactly the proportion of times it belongs to triangles formed by the epicenters of earthquakes. Of course, it is more reasonable to consider local depth functions instead of global ones. The choice of  $\tau$  is very important for local depth because it measures the size of the neighbourhood for the analysis. Again according the spatial distribution of epicenters, if we use the diameter to measure simplex size,  $\tau$  indicates the maximum distance (degrees) between the epicenters corresponding to simplex vertices. If we use the volume,  $\tau$  indicates the area of the simplex.

The first analysis we introduce here is the computing of global and local depth values of the capitals of Italian provinces with respect to the spatial distribution of epicenters. More specifically, we consider 103 towns and epicenters are represented as planar points. The error due to overlooking Earth's curvature is negligible. Table 9 shows three ranks of seismic risk for Italian towns, the first representing global depth values while the second and the third are local depth values corresponding to size of simplices measured by diameter and volume, respectively. The 5% percentile of the distribution of simplex diameters or volumes is used. Depth values returned in Table 9 are normalized as follows:

$$d^* = (d - d_{min}) / (d_{max} - d_{min}). \quad (4)$$

L'Aquila and Perugia have the two highest depth values, according to all analyses. L'Aquila is very near to the epicenter of an earthquake with (moment) magnitude 6.3 occurred in 2009. For the global analysis, cities with higher risk are mainly situated in the center of Italy, in particular it seems that L'Aquila and Perugia would be the centers and the "danger" decreases along any direction from these two towns. To compare global and local depth we use the Spearman correlation. This coefficient shows more important variations between global and diameter (.487), instead global and volume are more similar (.802), with few important variations. The main difference between global and local depth is observed in the Tyrrhenian coast which in the global analysis is more risky, while in the local analysis it does not appear in Table 9 with the exception of some Campanian cities with volume method. When studying the differences between diameter and volume it is possible to observe that in the first case Emilian cities assume a depth value higher than volume, while in the second Southern cities result more risky than diameter. Despite these differences, Spearman's rank correlation value (.776) suggests that diameter and volume are quite similar . A comparison is presented in Figure 10 representing maps of seismic risk for global and local simplicial depth: the darkest colors correspond to the highest depth values with the caveat that colors are



extended to the entire corresponding province. The same analysis was also performed on the spherical coordinates of epicenters and the results were very close to the planar analysis, indeed the correlation coefficient is almost equal to 1. In the analysis below only local depth functions are considered because with respect to depth functions, they return a more flexible ranking, possibly with multiple centers.

Of course, when using simplicial depth it is important to decide on a reasonable value of  $\tau$ . A possible criterion is given by Kolmogorov-Smirnov test of equality of local and global depth. Kolmogorov-Smirnov test is a nonparametric test used to check the statistical hypothesis that the samples are drawn from the same distribution. This test quantifies a distance between the empirical distribution functions of the reference sample. Figure 9 shows the results of the test for the comparison of global and local depth. Diameter has a pattern more similar to the global depth than volume. In fact, when using diameter, we keep rejecting the null hypothesis for quantile values of  $\tau$  not greater than 40%. Differently for volume we accept the hypothesis that the samples are drawn from the same distribution for  $\tau$  values greater than 70%.

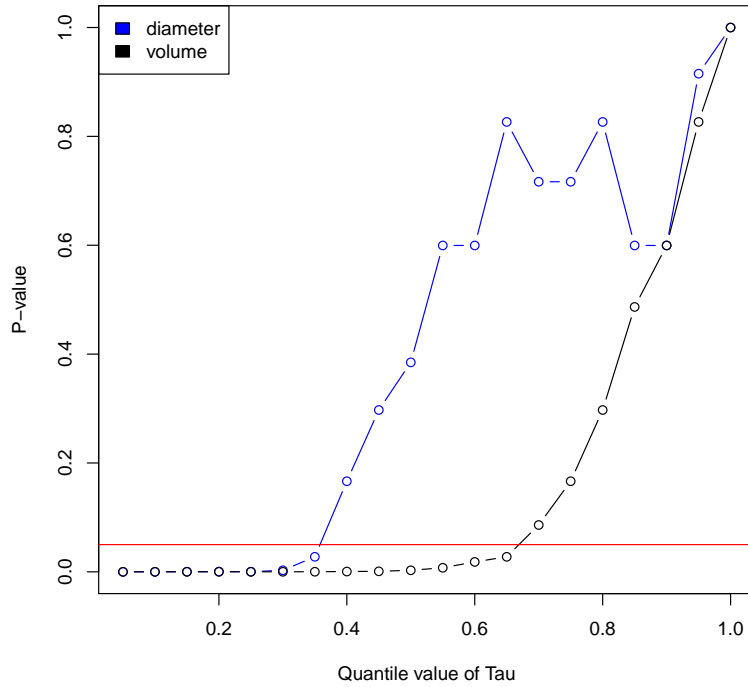


Figure 9: P-value of Kolmogorov-Smirnov test as a function of  $\tau$ , (horizontal line corresponds to 5%).

## 5.2 Spatial-Magnitude Analysis

Previous results only consider the spatial distribution of epicenters. In this section we add magnitude in the local depth analysis. Particularly, we illustrate the results by means of seismic risk for different values of magnitude. Figure 11 and 12 represent maps of seismic risk according to local depth using as a measure of simplex size diameter and volume, respectively. The Italian maps are colored with different levels of gray, with darker shades of gray corresponding to higher depth values or risk. Note that gray scale is conditional on each magnitude class, this implies that the same gray level in different maps do not mean equal depth values, but rather equal depth values conditional on magnitude classes. For example, if a region is colored black with a value of magnitude and varying it in other regions colored in black does not mean that the value of depth is the same, but only that the value for that map is the most risky. A particular variation pattern is suggested by the comparison of Figures 11 and 12. Lower magnitude events are mainly concentrated in the North and Center of Italy, whereas when magnitude increases the more risky areas are in the South of the country. The behavior for diameter and volume is similar, indeed Spearman's rank correlation is about 0.94. The main difference between the two measures of simplex size is that for lower magnitude values North-East regions of Italy are more risky according to diameter then volume. For higher magnitudes, diameter emphasizes Calabrian cities and Messina while volume emphasizes more Campanian towns.

# Appendix A: conditional distribution of century and magnitude

1600 - 1700				
	Magnitude			
Region	[4.5-4.81] %	(4.81-4.83] %	(4.83-5.17] %	(5.17-7.41] %
1	0.93(1)	0(0)	0.93(1)	2.78(3)
2	0.47(1)	0.47(1)	2.33(5)	0.93(2)
3	0.78(2)	2.72(7)	1.95(5)	2.72(7)
4	0.52(2)	0.78(3)	1.31(5)	0.78(3)
5	1.12(1)	1.12(1)	3.37(3)	2.25(2)
6	0(0)	2.22(2)	0(0)	2.22(2)
7	0(0)	0.53(1)	2.63(5)	2.63(5)
8	0(0)	1.46(2)	0.73(1)	2.92(4)
1700 - 1800				
	Magnitude			
Region	[4.5-4.81] %	(4.81-4.83] %	(4.83-5.17] %	(5.17-7.41] %
1	0(0)	0(0)	1.85(2)	2.78(3)
2	6.51(14)	1.86(4)	3.26(7)	2.79(6)
3	0.39(1)	1.95(5)	2.72(7)	4.67(12)
4	0(0)	3.13(12)	6.79(26)	4.18(16)
5	0(0)	0(0)	3.37(3)	4.49(4)
6	0(0)	2.22(2)	2.22(2)	3.33(3)
7	2.63(5)	3.16(6)	5.26(10)	5.26(10)
8	0(0)	0.73(1)	2.92(4)	5.11(7)
1800 - 1900				
	Magnitude			
Region	[4.5-4.81] %	(4.81-4.83] %	(4.83-5.17] %	(5.17-7.41] %
1	3.70(4)	20.37(22)	6.48(7)	9.26(10)
2	7.44(16)	7.91(17)	13.02(28)	3.26(7)
3	3.89(10)	8.95(23)	8.56(22)	6.61(17)
4	3.66(14)	8.09(31)	7.83(30)	4.44(17)
5	2.25(2)	5.62(5)	10.11(9)	10.11(9)
6	2.22(2)	5.56(5)	7.78(7)	8.89(8)
7	2.63(5)	11.58(22)	8.42(16)	5.79(11)
8	5.84(8)	4.38(6)	8.03(11)	5.11(7)
1900 - 2300				
	Magnitude			
Region	[4.5-4.81] %	(4.81-4.83] %	(4.83-5.17] %	(5.17-7.41] %
1	22.22(24)	10.19(11)	8.33(9)	10.19(11)
2	20.00(43)	10.23(22)	12.56(27)	6.98(15)
3	19.84(51)	10.51(27)	12.45(32)	11.28(29)
4	19.58(75)	16.71(64)	15.40(59)	6.79(26)
5	14.61(13)	16.85(15)	15.73(14)	8.99(8)
6	14.44(13)	21.11(19)	15.56(14)	12.22(11)
7	16.32(31)	12.11(23)	11.05(21)	10.00(19)
8	21.90(30)	17.52(24)	11.68(16)	11.68(16)

Table 8: Conditional distribution of century and magnitude, given the tectonic region. Layout as in Table 4.

## Appendix B: global and local depth values of spatial analysis

Province capital	D (RANK)	Province capital	LDD (RANK)	Province capital	LDV (RANK)
L'Aquila	1.0 (103)	L'Aquila	1.0 (103)	L'Aquila	1.0 (103)
Perugia	.954 (102)	Perugia	.829 (102)	Perugia	.664 (102)
Rieti	.946 (101)	Bologna	.651 (100.5)	Terni	.571 (101)
Terni	.933 (100)	Modena	.651 (100.5)	Rieti	.557 (100)
Arezzo	.849 (99)	Forlì	.588 (99)	Forlì	.442 (99)
Frosinone	.835 (98)	Arezzo	.552 (98)	Arezzo	.363 (98)
Isernia	.780 (97)	Reggio Emilia	.532 (97)	Isernia	.353 (97)
Caserta	.741 (96)	Terni	.486 (96)	Firenze	.307 (96)
Ascoli Piceno	.737 (95)	Rieti	.446 (95)	Vibo Valentia	.297 (95)
Napoli	.733 (94)	Mantova	.420 (94)	Prato	.278 (94)
Teramo	.724 (93)	Firenze	.372 (93)	Catanzaro	.268 (93)
Firenze	.713 (92)	Vibo Valentia	.362 (92)	Parma	.253 (92)
Prato	.655 (91)	Ascoli Piceno	.359 (91)	Reggio Calabria	.241 (91)
Benevento	.639 (89.5)	Messina	.356 (90)	Ascoli Piceno	.237 (90)
Salerno	.639 (89.5)	Macerata	.355 (89)	Pistoia	.235 (88.5)
Avellino	.638 (88)	Ferrara	.351 (88)	Messina	.235 (88.5)
Macerata	.635 (87)	Prato	.313 (87)	Benevento	.220 (87)
Forlì	.629 (86)	Parma	.308 (86)	Ancona	.208 (86)
Pistoia	.599 (85)	Verona	.284 (85)	Modena	.201 (85)
Latina	.592 (84)	Teramo	.278 (84)	Reggio Emilia	.189 (84)
Pesaro Urbino	.579 (83)	Isernia	.263 (83)	Bologna	.181 (83)
Campobasso	.570 (82)	Rovigo	.224 (82)	Teramo	.169 (82)
Viterbo	.563 (81)	Padova	.195 (81)	Foggia	.164 (81)
Siena	.562 (80)	Vicenza	.193 (80)	Frosinone	.151 (80)
Rimini	.559 (79)	Campobasso	.191 (79)	Campobasso	.140 (79)
Pescara	.549 (78)	Reggio Calabria	.170 (78)	Macerata	.139 (78)
Ravenna	.529 (77)	Foggia	.164 (77)	Caserta	.137 (77)
Bologna	.517 (76)	Pistoia	.162 (76)	Potenza	.130 (76)
Roma	.515 (75)	Pesaro Urbino	.139 (75)	Ferrara	.112 (75)
Ancona	.514 (74)	Ancona	.124 (74)	Napoli	.106 (74)

Table 9: Depth values and ranks of the upper quartile of province capitals (D: global simplicial depth; LDD: local simplicial depth, diameter version; LDV: local simplicial depth, volume version).

## Appendix C-1: maps of spatial analysis

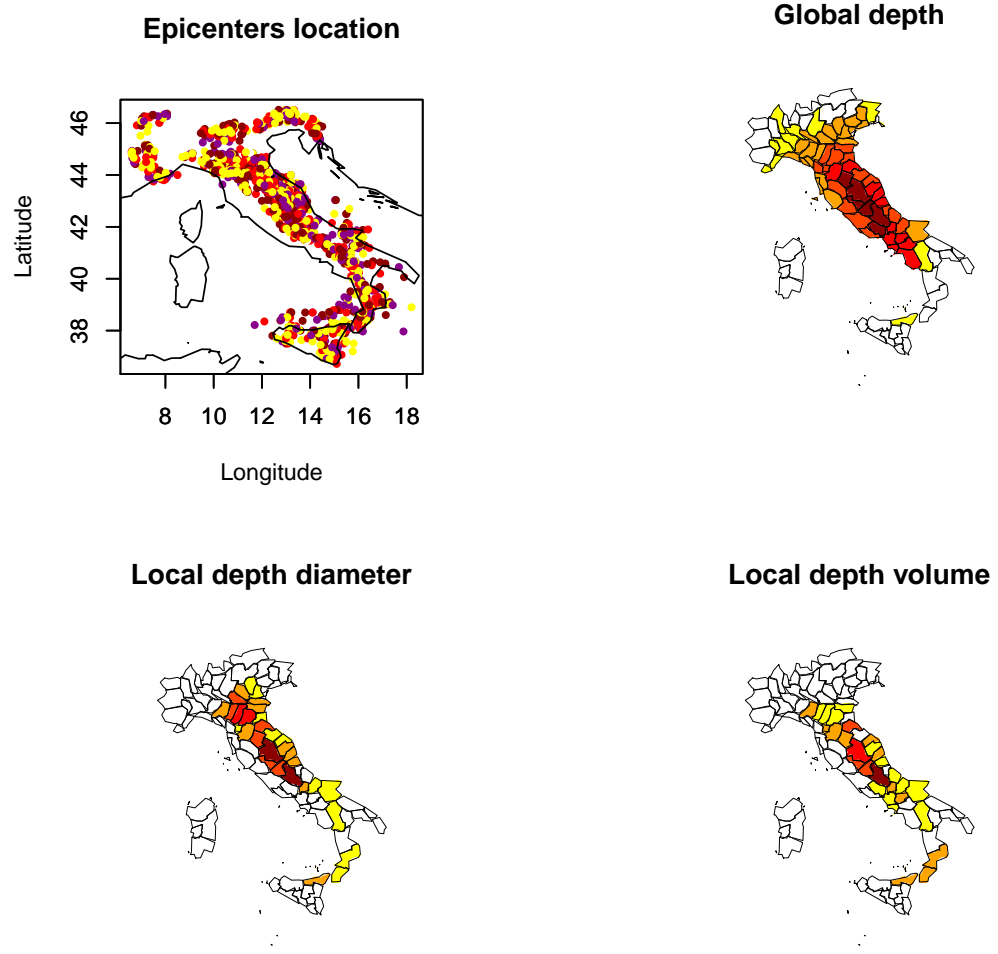


Figure 10: Maps of seismic risk. Top left: map of epicenters with colors correspond to magnitude; top right: global simplicial depth; bottom left: local simplicial depth, diameter version; bottom right: local simplicial depth, volume version;  $\tau$ : 5% percentile of triangle diameters or areas.

Appendix C-2: maps of spatial-magnitude analysis

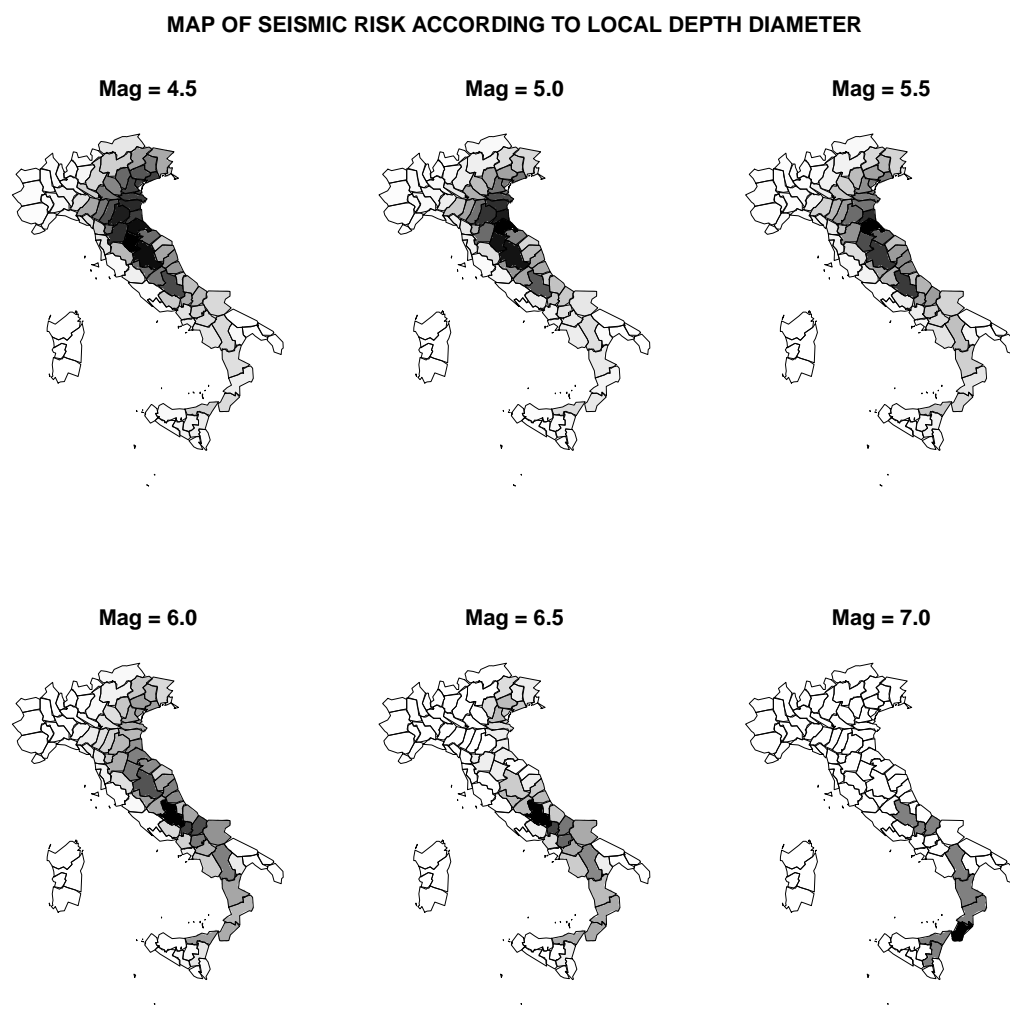


Figure 11: Maps of seismic risk.

**MAP OF SEISMIC RISK ACCORDING TO LOCAL DEPTH VOLUME**

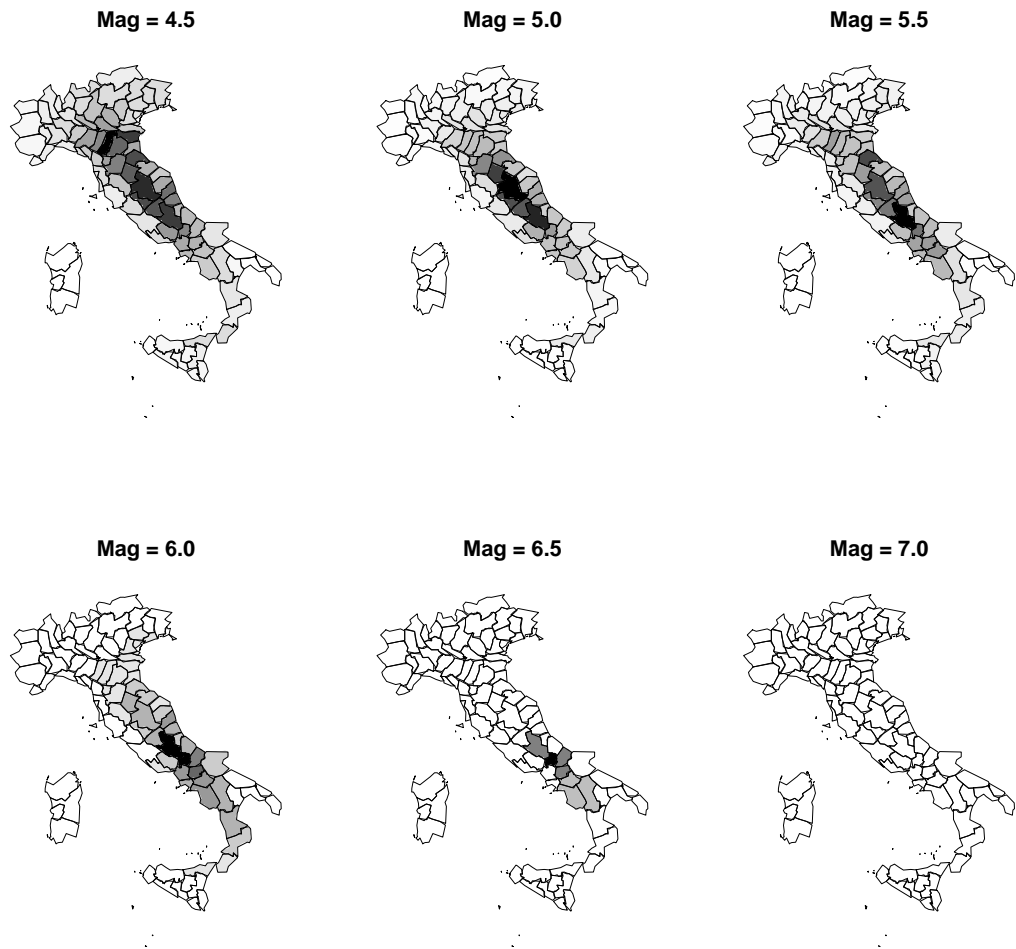


Figure 12: Maps of seismic risk.

## References

- Agostinelli C, Romanazzi M (2011) Local depth. *Journal of Statistical Planning and Inference* 141:817–830
- Gutenberg B, Richter CF (1956) Earthquake magnitude, intensity, energy, and acceleration (second paper). *Seismological Society of America Bulletin* 46:105–145
- Hanks T, Kanamori H (1979) A moment magnitude scale. *J Geophys Res* 84:2348–2350
- Hutton K, Woessner J, Hauksson E (2010) Earthquake monitoring in southern california for seventy-seven years (1932-2008). *Bulletin of the Seismological Society of America* 100:423–446
- Liu RY, Parelius JM, Singh K (1999) Multivariate analysis by data depth: descriptive statistics, graphics and inference. *The Annals of Statistics* 27:783–858
- Richter CF (1935) An instrumental earthquake magnitude scale. *Bulletin of the Seismological Society of America* 25:1–32
- Rosenblatt M (1956) Remarks on some nonparametric estimates of a density function. *Ann Math Statist*, Number 3 27:832–837
- Small CG (1990) A survey of multidimensional medians. *International Statistical Review* 58:263–277
- Woessner J, Hardebeck J, Hauksson E (2010) What is an instrumental seismicity catalog. *Community Online Resource for Statistical Seismicity Analysis*